MECHANICAL INSTABILITY AND YIELDING OF POLYCARBONATE

HIGUCHI, Masakazu
Research Institute for Applied Mechanics, Kyushu University : Professor

HYAKUTAKE, Hiizu
Fukuoka University : Assistant Professor

https://doi.org/10.5109/7170826

出版情報：Reports of Research Institute for Applied Mechanics. 16 (54), pp.265-282, 1968. 九州大学応用力学研究所
バージョン：
権利関係：

Reports of Research Institute for Applied Mechanics
Vol. XVI, No. 54, 1968

MECHANICAL INSTABILITY AND YIELDING OF POLYCARBONATE

By
Masakazu HIGUCHI* and Hiizu HYAKUTAKE**

To investigate the mechanical behavior and to determine the criterion for necking of polycarbonate, static tests of several loading conditions (tension, compression, torsion and internal pressure test of thin-walled cylinders) have been carried out at room temperature. Sequence photography was used and careful observation was made in conjunction with the load-deformation measurement.

The mechanical properties in each test were compared with one another in the terms of the equivalent stress and strain. The equivalent strain at the maximum load of tension is lower than that at the maximum torque in torsion test. The former is the strain of mechanical instability, analogous to necking of metals, and the latter the strain at 'yielding' of polycarbonate. There have been also examined deformation bands initiation in the material.

1. Introduction.

Polycarbonate, a kind of thermoplastics, posseses very interesting properties characterized especially by high impact resistance in a low temperature range as well as good rigidity and dimensional stability.[1] Since Hechelhammer and Peilstoecker[2] investigated on physical and chemical properties of polycarbonate, much experimental work has been done; Robertson and Buenker [3] examined the change in modulus with the degrees of orientation. Ekval and Low [4] measured the temperature dependence of tensile properties. Robertson [5] studied on the shape of neck in cold-drawing. Mercier et al. [6] investigated the viscoelastic properties. Recently Higuchi [7] has studied on the fatigue fracture and Maeda et al. [8] reported the work on plastic forming at room temperature.

The present work is devoted to the study of mechanical behaviors at room temperature and to revealing the interrelationship of yielding, necking and cold-drawing of polycarbonate. When rigid plastics such as polycarbonate are subjected to tension, the load rapidly declines at a strain of a few percent, and then necking and cold-drawing successively occur. These processes were explained by Marshal et al., [9] relying on a mechanism of softening due to localized heating; the mechanism might be capable to explain

* Professor, Member of Research Institute for Applied Mechanics, Kyushu University.
** Assistant Professor of Fukuoka University.

one of the phenomena, necking, but not its propagation, the cold-drawing. Vincent [10] gave another sort of explanation from a standpoint of mechanical instability. This follows the Considère's construction on the stress-strain curve, and has recently been supported by Argon et al., [11] who on the occasion used a term material instability to indicate yielding of polymers.

In order to know the material properties as a function of the strain and especially of the true stress in the immediate vicinity of the maximum load, we have examined the stress-strain relations in several statical loading conditions (tension, compression, torsion and internal pressure in thin-walled cylinders), and carefully determined the points of neck formation on the stress-strain curves obtained. To make clear the relation between neck formation and deformation bands appearance, sequence photographs were taken and observation was made in conjunction with the measurement of the values of stresses and strains.

2. Specimens.

Polycarbonate used was of commercial grade, purchased from the market. The materials were 5 mm thick plates and circular rods 20 mm and 30 mm in diameter. The plates in the as-received condition were free of birefringence whereas the rods showed some.

Specimens, after machining, were meticulously polished and buffed by a standard metallographic technique. Prior to testing they were heat-treated in a silicone oil bath of 140°C for 5 hours and cooled at a rate of 0.1°C/min. With this treatment, the residual stresses in the specimens were mostly eliminated and the specimens hardly changed their volume. [12]

Table 1.

Specimen Direction	Maximum Stress (kg/mm^2)
0°	7.33
15°	7.36
30°	7.26
45°	7.32
90°	7.27

The plates had no intrinsic anisotropy; the flat tensile specimens were so taken from a plate material that the directions of their length made angles of 0°, 15°, 30°, 45° and 90° with the longitudinal direction of the plates; the stresses and strains at maximum load were found almost equal to one another value through a preliminary measurement (Table 1).

All of the measurements have been made under the condition of 23 ± 1°C and 50 ± 3 %RH.

3. Measurement and Observation.

3-1 Tension Test.

3-1-1 Tension Test of Flat Specimens.

The dimensions of the specimens are given in Fig. 1. A typical one of the graphs of tensile load against extension is shown in Fig. 2, being reproduced from a chart paper record. The selected crosshead speeds were mostly 0.5 mm/min. Crazes presenting a silky appearance became discernible in the vicinity of the point A on the graph shown in Fig. 2. Crazes often grew up from faint polish scratches left on the surfaces and, if any, on fingered portions. The magnitude of the strain to initiate crazing was observed to be the more and the craze density the less with the higher rate of straining, similarly to the results obtained with other polymers.[13] Beyond the point B on the curve the load begins to decrease gradually. Just after that, fine deformation bands are appreciably produced both on the specimen surface and in its interior with decrease in load.

Sequence photographs of the specimen were taken using a 35 mm camera

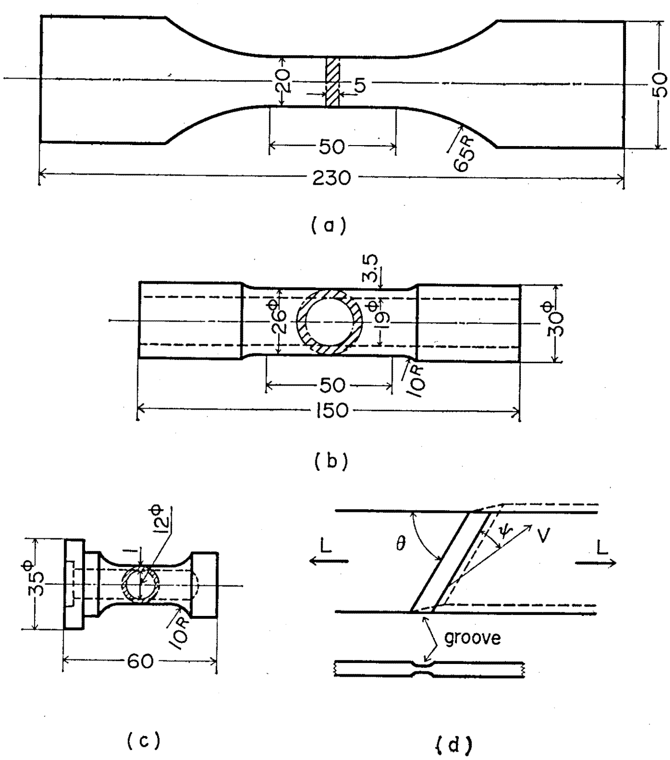

Fig. 1. Specimens for (a) tension, (b) torsion, (c) internal pressure test, and (d) a grooved specimen.

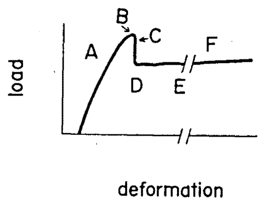

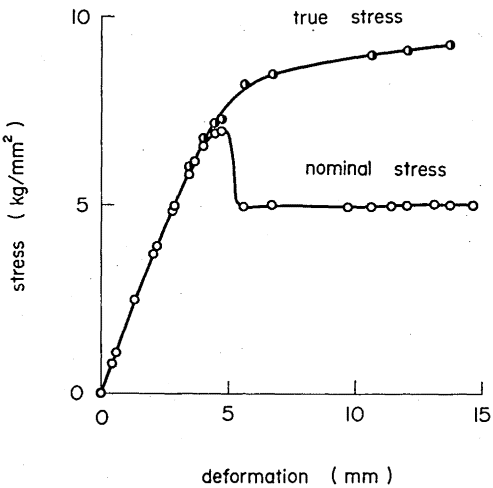

Fig. 2. (Upper right) Load-extension curve of a flat tensile specimen. Velocity of extension is 0.5 mm/min.

Fig. 3. True stress-strain curve of a flat tensile specimen.

at intervals of 2 seconds, over the period from B to E, and reproduced in Fig. 4. There is seen no appreciable deformation in the specimen yet at C beyond the maximum load in the stress-strain diagram. A shadow, which appeared at the stage C and is indicated by an arrow in the photo, was composed of a crowd of X-type short deformation bands in the inside; at this area successively occurs the necking. This develops in a direction making an angle of 59~63 degrees with the axis of extension (Fig. 4b). It comes under our notice that the geometry of the neck in polycarbonate is remarkably similar to that of mild steel, for a tensile flat specimen of which the incipient plastic constriction has been explained to develop along a narrow band in such a direction as the normal strain to vanish and the direction is calculated to be 54°44′ with the tensile axis.[14] Beyond the stage D of the least load, the necked part continuously spreads with elongation under the constant load; this is the process of cold-drawing of polycarbonate, during which the shoulders of the neck travel along the specimen and the strain in the necked part remains in the range of 0.7~0.8 regardless of the elongation of the specimen. As the necked part covers over the specimen, the tensile load gradually begins to increase.

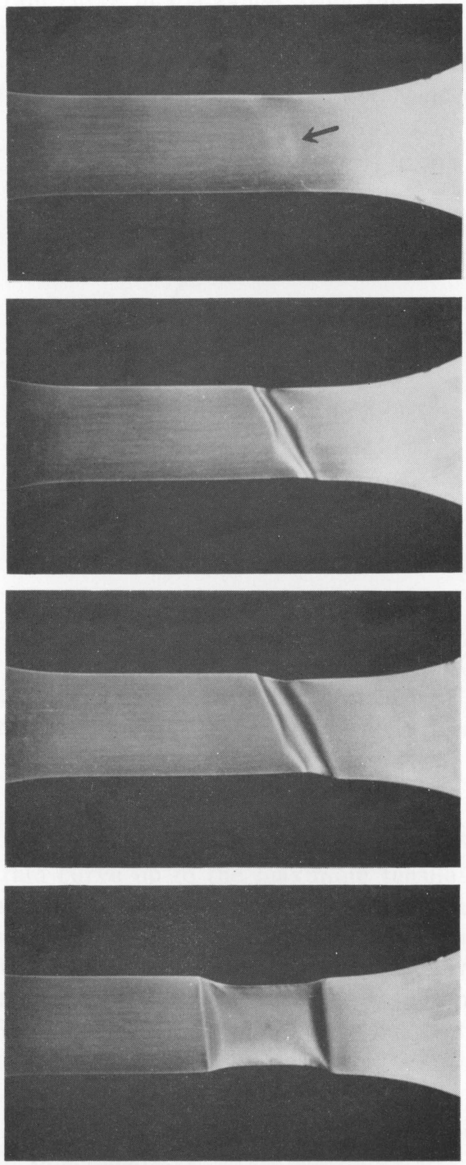

Fig. 4. Neck growth in a flat tensile specimen.
(a) Deformation bands initiation at C in Fig. 2.
A shadow shown by an arrow is an area containing a crowd of deformation bands.
(b) Neck formation after 2 seconds from (a).
(c) Neck growth after 48 seconds.
(d) Cold-drawing at E in Fig. 2.

(*Facing p.* 268)

A true stress-strain curve in the range from the stage of the maximum load to the cold-drawing has been obtained from the load-extension curve by aid of the sequence photograph and is shown in Fig. 3. It is known that the true stress is monotonically increasing with the extension of the specimen.

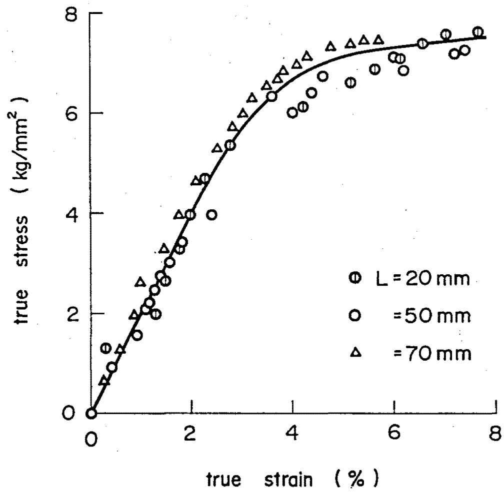

Fig. 5. True stress-strain curve of rod specimens.

Fracture was caused by a fine flaw in the necked part after it had grown up to such a diamond-type crack (Fig. 8) as had been observed in polymethyl methacrylate.[15]

3-1-2 Tension Test of Rod Specimens.

A true stress-strain curve up to the maximum tensile load was obtained from the data of circular rod specimens, which were 10 mm in diameter and 20, 50 and 70 mm in gauge length. The strain rate of about 10^{-4}/sec was used. The strains were obtained from telescopic measurement of the changes in distance of gauge lines on the specimens. The results of the measurement are shown in Fig. 5. The stress-strain behavior is nearly linear up to a stress of about 4 kg/mm². The tensile load reached the maximum at a strain of about 7 %.

3-1-3 Strain Rate Dependence.

The strain rate dependence of the mechanical behaviors such as the stress-strain curve, time of crazing, deformation bands initiation and necking formation was examined with plate specimens. The dimensions of the specimens were 5 mm thick, 15 mm wide and 40 mm in gauge length. The rates of straining were in the range of $1.72 \times 10^{-6} \sim 1.55 \times 10^{-2}$/sec. Like with other polymers, the stress and strain at the maximum tensile load increase with the strain rate (Fig. 6).

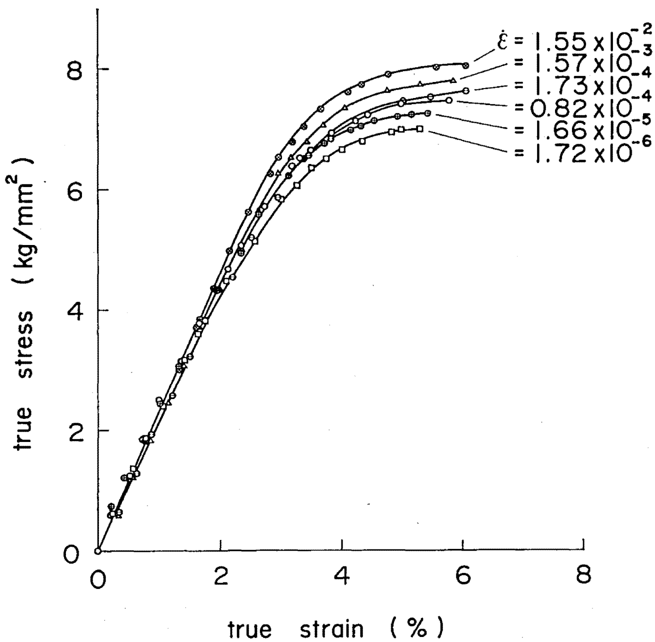

Fig. 6. True stress-strain curves at different tensile strain rates.

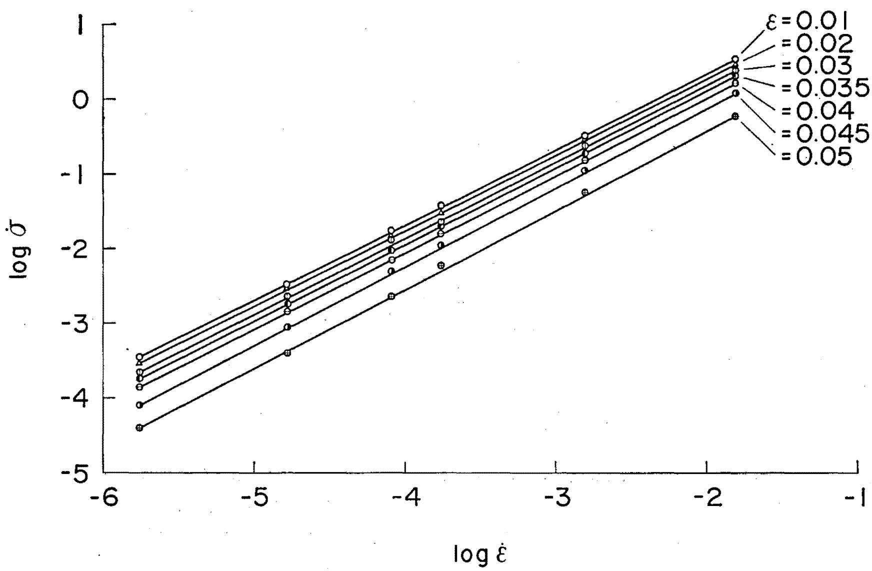

Fig. 7. Relation of stress rates and strain rates obtained from the data presented in Fig. 6.

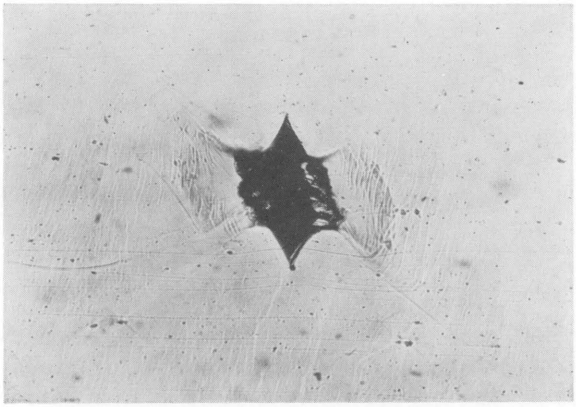

Fig. 8 Diamond-type crack in a necked part of a tensile specimen (50×).
Tensile direction is lateral.

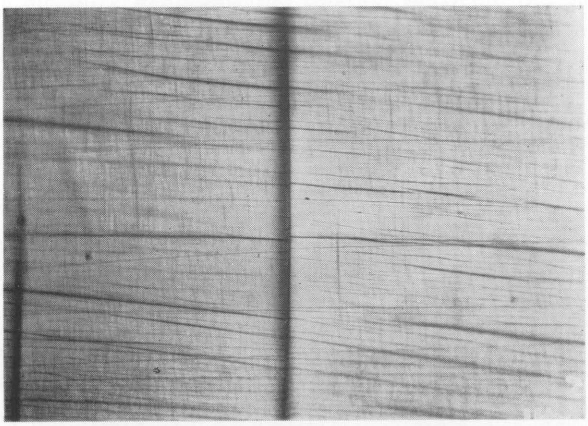

Fig. 9. Deformation bands produced at maximum torque (50×).
Axis of torsion is horizontal. Circumferential (vertical) bands are seen produced later.

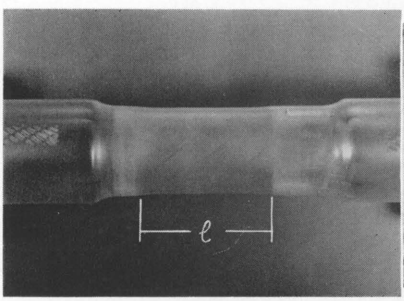

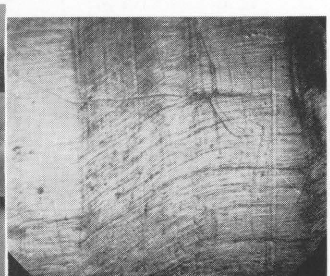

Fig. 10. Torsional-necked specimen.
Left after propagation.
Right boundary between necked and un-necked (20×).

(*Facing p.* 270)

The data can be represented as

$$\sigma = A\varepsilon + B\varepsilon^n \tag{1}$$

under the condition of non-decreasing load. A rheological equation of Knowles et al.[16] is too complicated for our purpose to evaluate the stress of instability by Considère's construction. The strain at maximum load, ε_0, is derived from the equation (1) as

$$\varepsilon_0 = \left(-\frac{A}{nB}\right)^{1/(n-1)} \tag{2}$$

A, B and n, depending on the strain rate, have been determined for the data to fit the equation (1) well especially in the upper range. The evaluated values of ε_0 are presented in Table 2. With the increase in strain rate, the stress for deformation bands initiation was raised and the bands density decreased.

In addition we have examined the relation between the stress rate and the strain rate in tension test. The stress rate $\dot{\sigma}$ is related to the strain rate $\dot{\varepsilon}$ as

$$\dot{\sigma} = \frac{\Delta\sigma}{\Delta t} = \frac{\Delta\sigma}{\Delta\varepsilon}\cdot\frac{\Delta\varepsilon}{\Delta t} = \frac{\Delta\sigma}{\Delta\varepsilon}\cdot\dot{\varepsilon} \tag{3}$$

Table 2.

Strain Rate	Constants in Eq. (1)			Strain at the maximum load	
	A	B	n	Measured (%)	Evaluated (%)
1.72×10^{-6}	220.4	-1.057×10^{4}	2.632	4.97	5.16
1.66×10^{-5}	220.4	-0.905×10^{4}	2.597	5.16	5.37
0.82×10^{-4}	220.4	-1.223×10^{4}	2.721	5.28	5.42
1.73×10^{-4}	220.4	-1.029×10^{4}	2.667	5.50	5.53
1.57×10^{-3}	220.4	-1.588×10^{4}	2.837	5.31	5.52
1.55×10^{-2}	220.4	-3.153×10^{4}	3.101	5.57	5.50

For each value of $\dot{\varepsilon}$, the stress increment $\Delta\sigma$ per strain increment $\Delta\varepsilon=0.5\,\%$ (say) were measured with dividers on the stress-strain curve in Fig. 6. Plot of $\log\dot{\sigma}\sim\log\dot{\varepsilon}$ has been tried[17] and found remarkably linear and parallel to one another (Fig. 7).

3-2 Torsion Test.

3-2-1 Torsion Test of Thin-Walled Cylinders.

The shape of the specimens is illustrated in Fig. 1. A typical one of the graphs of the moment against the angle of twist, which was obtained by measuring the angle between the grips, is shown in Fig. 11. The angular velocity of the grip was set at 15 deg/min. The testing machine is so designed that one of the grips can move freely along the moment axis.

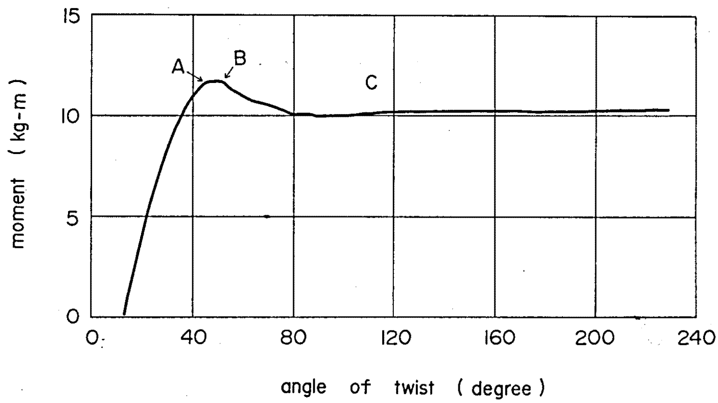

Fig. 11. Torsion of a thin-walled cylinder.

Deformation bands begin to appear, just when the moment reached the maximum, along the planes of maximum shear stresses (Fig. 9). They rapidly develop under the constant moment, and after this stage the moment abruptly drops to a value as seen in Fig. 11, in which process the specimen diminishes in diameter at a localized section of a few millimeter length where the material a little recovers the transparency having been lost due to the initial deformation bands growth, but has been found to have had much dense deformation bands produced there. The diminution in diameter ceases at the point C in Fig. 11, and then the shoulders of the neck travel along the specimen axis under the constant moment (Fig. 10). The material is now cold-drawing.

3-2-2 Torsion Test of Solid Bars.

A stress-strain curve up to the maximum torque was obtained with solid circular specimens. We prepared two of specimens which had the same dimensions but the gauge length. They were 20 mm in diameter; 5 mm and 41 mm in gauge length. With these, eliminating the end effect from the measurements of the angles between the grips, we obtained a diagram of moment against angle of twist per unit length, and following the method of Hill,[18] derived the relation of stress and strain of uniform values (Fig. 12).

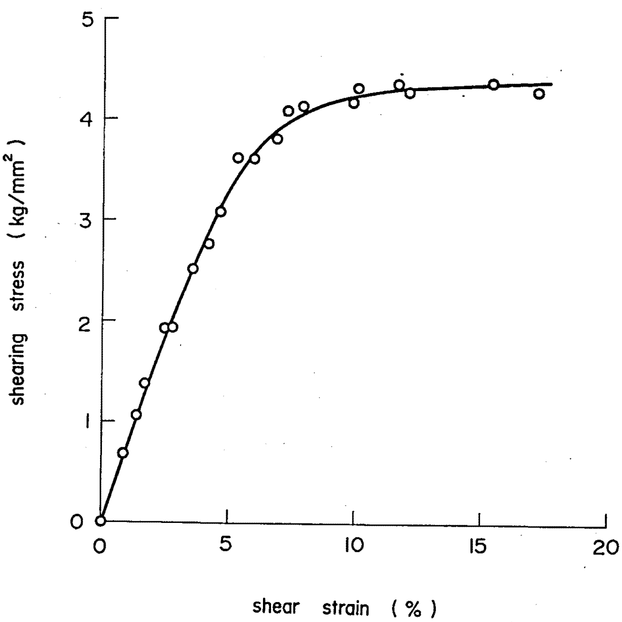

Fig. 12. Uniform stress vs. strain of shearing.

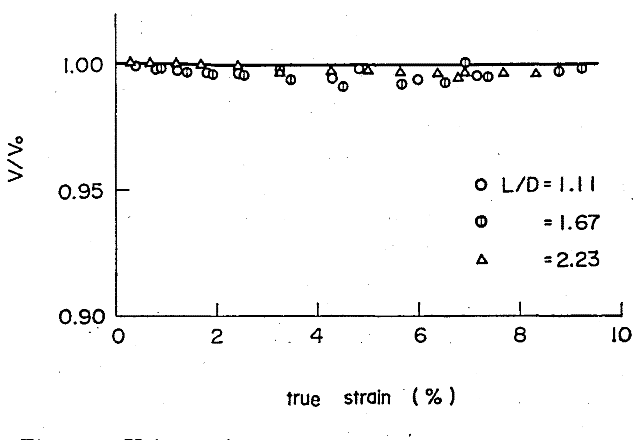

Fig. 13. Volume change vs. true compressive strain.

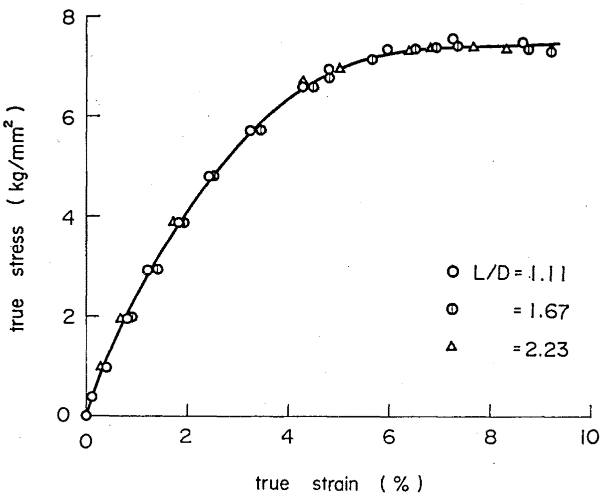

Fig. 14. True stress-strain curve in compression.

3-3 Other Tests.

3-3-1 Compression Test.

Cylindrical specimens of 18 mm in diameter were prepared for compression test. The height to diameter ratios were 1. 11, 1. 67 and 2. 23. The strains were obtained by measuring the changes in diameter and height of the specimens. Concentric grooves had been cut on the end surfaces and tried to eliminate the effect of friction arising between the anvils and the specimen following the method of Loizou et al.[19] A few trial tests had been performed with different shapes and numbers of grooves. But they failed because deformation bands were produced from the edges of the grooves (Fig. 15), and gave another trouble to the evaluation of the depth change. We have after all done without grooves.

The anvil faces and the end surfaces of the specimens were meticulously polished and were well lubricated with a mixture of grease and graphite. The measurements of the volume of a not grooved specimen are plotted against strains (Fig. 13). After unloading, the specimen was cut into round slices. The isochromatic fringe photographs of the slices from the various parts are reproduced in Fig. 16. They differ little from one another and show the absence of deformation localized at the specimen end.

The stress-strain curve forms just as in the true stress-strain curve for tension (Fig. 14). Getting to the maximum load, the load remains stable for a while, after which the uniformity of deformation of the specimen begins to break. However, the specimens differ with those subjected to tension in that they give rise, when unloaded immediately after the arrival at the

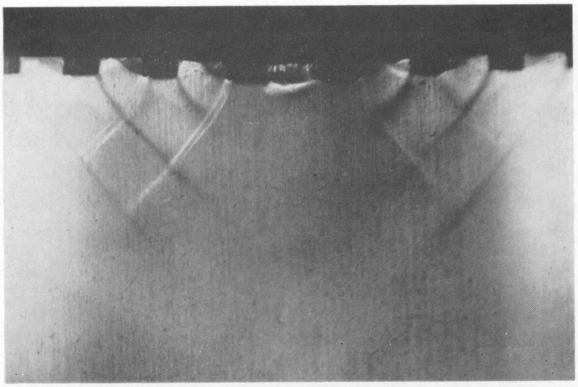

Fig. 15. Deformation bands produced at a grooved specimen end (5×).

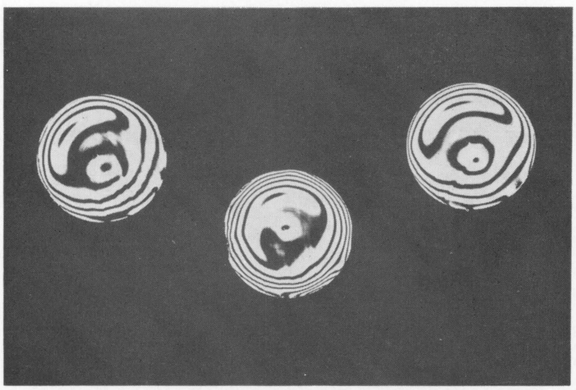

Fig. 16 Isochromatic fringes in compression specimen slices.

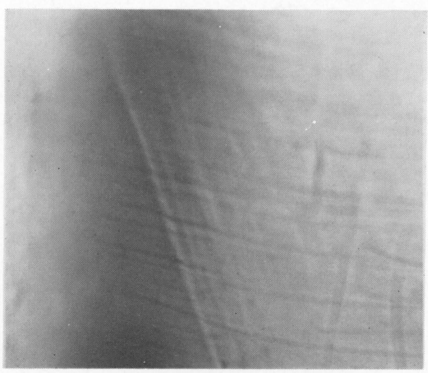

Fig. 17 Deformation bands produced in the inside of compression test specimen (5×).

(*Facing p.* 274)

maximum load, to undulations on the polished and heat-treated face of the axial section. The undulations stretch at an angle of $26° \sim 30°$, considering the elastic recovery, to the loading axis (Fig. 17). We construe them as an assemblage of numerous small bands. Although fine deformation bands have been observed by Argon et al. soon to appear in the stage of deviation of the load-contraction relation from the linearity, it has been done with notched specimens. We do not think such is the case when consideration is taken of the stress value at the notch bottom and the true stress-strain curve is drawn of the local values.

3-3-2 Internal Pressure Test of Thin-Walled Cylinders.

The dimensions of specimens are shown in Fig. 1. The axial and radial displacements were measured at the same time as the internal pressure measurement, from which the three principal strain ε_t, ε_r and ε_z in tangential, radial and axial directions respectively were calculated as

$$\varepsilon_t = \ln D/D_o, \quad \varepsilon_z = \ln l/l_o, \quad \varepsilon_r = -(\varepsilon_t + \varepsilon_z), \tag{4}$$

where D is the diameter and l the gauge length. The subscript o denotes the initial values of them. When localized bulging occurred at a part of the wall the pressure began to decrease. The equivalent stress and strain were calculated from the formulas,

$$\bar{\sigma} = \frac{\sqrt{3}}{2} \cdot p \frac{D}{2t}, \quad \bar{\varepsilon} = \sqrt{\frac{2}{3}(\varepsilon_t^2 + \varepsilon_z^2 + \varepsilon_r^2)}, \tag{5}$$

p, t being the internal pressure and the wall thickness (Fig. 18). The values

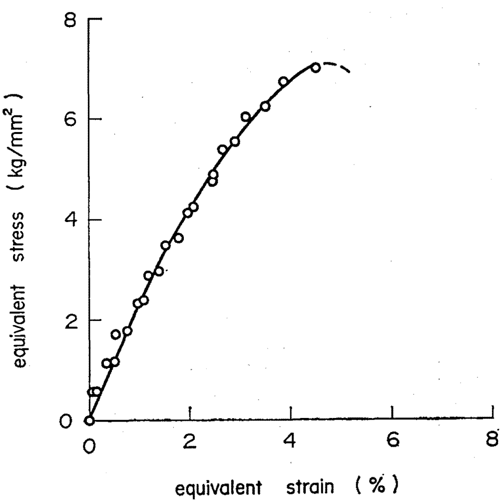

Fig. 18. Equivalent stress vs. equivalent strain in internal pressure test.

of the stress and strain are the larger for the higher rates of straining.

3-3-3 Tension Test of Grooved Plates.

Hill [20] suggested the use of grooved tensile specimens to examine the deformational instability in biaxial stress states. Fig. 1 shows the form of the specimens; θ is the angle indicating the direction of grooves and ψ is the angle of the direction V for the right part to leave the left half. The cases of $\theta=54°44'$ and 90° give the identical states of stresses with those in a plate specimen with no groove and in a thin-walled cylinder subjected to internal pressure respectively. [21][22][23]

The results of the tension tests [24] for $\theta=55°$ to 90° are shown in Fig. 19 with vectorial representation on the π plane [25] of the deviatoric stresses at the maximum load. A circle indicating the von Mises' yield criterion for mild steel is represented together with the stresses in simple tension as well as in internal pressure test.

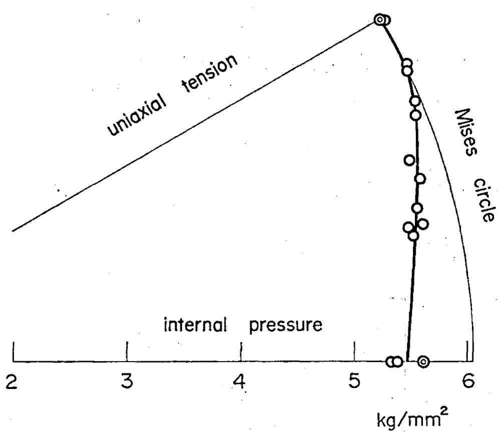

Fig. 19. Vectorial representation of necking stresses.

4. Deformation bands.

Whitney first noticed deformation bands of polystyrene. [26] Newman et al. [27] earlier observed flow lines in polymethyl methacrylate. Both may be of the same nature. For polycarbonate, we are understanding the deformation bands to be those shown in the photos of Figs. 20 through 25. Some of them are produced early before attaining the maximum load, undoubtedly because of a defect or some other stress raiser. In general they do not appear yet at maximum load of tension, neither in the stage of gently decreasing after the maximum. There were found no bands appeared when the load was removed as soon as it had ceased rising and begun to remain on

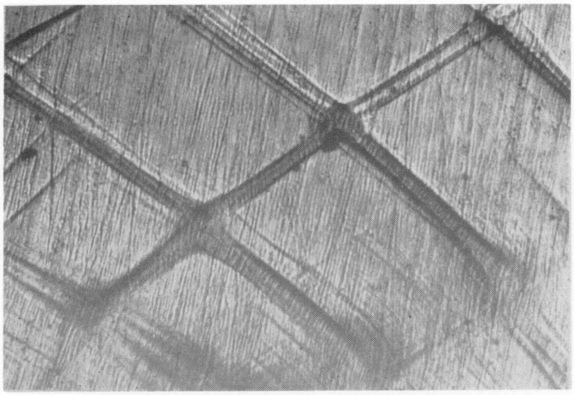

Fig. 20. Deformation bands in the inside of a tensile flat specimen (60×).
Load direction is vertical.

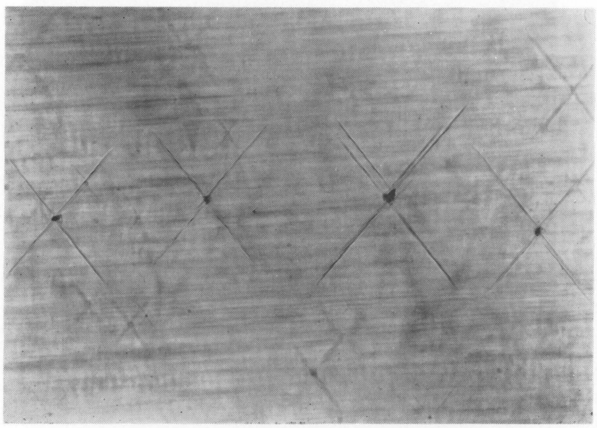

Fig. 21. X-type fine deformation bands (50×).
Horizontal tensile load.

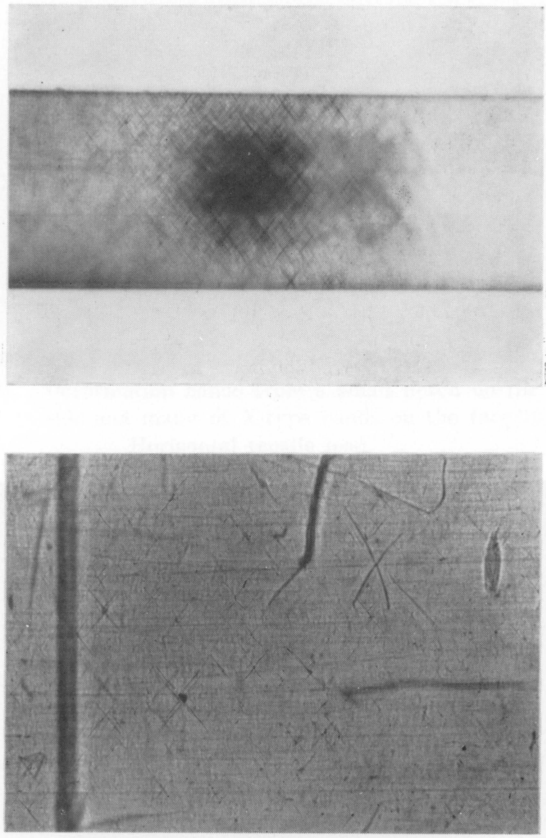

Fig. 22. X-type deformation bands grown in crowds in the stage C in Fig. 2 and (a) in Fig. 4.
Laterally (upper, 5 ×) and flatwise (10×) viewed.

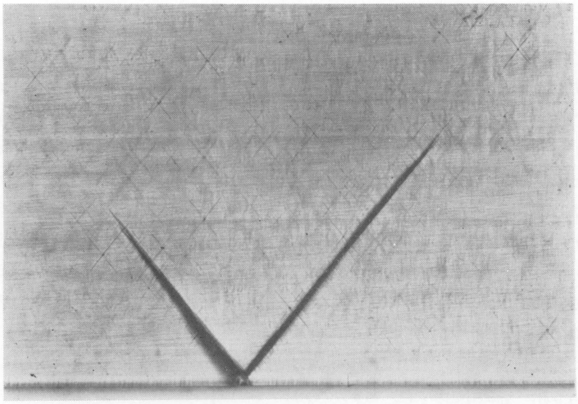

Fig. 23. Deformation bands from a small notch on the lateral side and many of X-type bands on the face(10×). Horizontal tensile load.

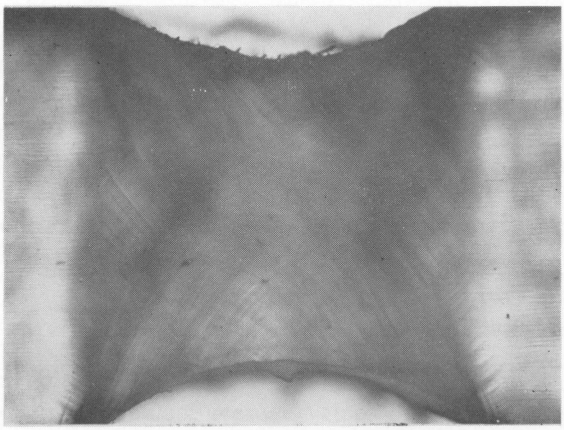

Fig. 24. 'Yielded' under tension(25×).

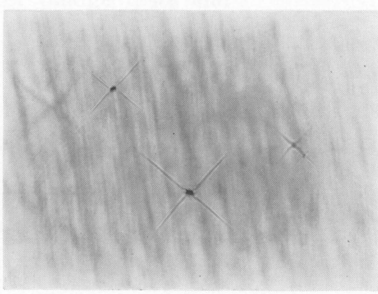

Fig. 25. X-type deformation bands produced under tension(30×).
An example of an angle different from that of Fig. 21.

the same level of the maximum. They appear simultaneously with a sudden drop of the load after subsequent incubation period. Fig. 20 shows the deformation bands in the interior of a specimen which was obtained according to the method of Argon et al. ; the specimen was sectioned parallel to its axis and annealed in a silicone oil bath of 140°C to produce the surface relief after the exposed face had been polished and buffed; we see the bands run at about 55° to the direction of tensile stresses. The angle 54°44′, though it has been mentioned as an angle of the neck in Section 3-1-1, is very near to this. On the other hand it is equal to an angle between a diagonal and an axis of a cuboid. It seems that Fig. 21 just shows such pairs of diagonals with each defect at each center, and from Figs. 21, 22, 23 that such cubic lattices are located as their faces to coincide with the specimen surface.

When the bands are multiplied and well developed, they present such appearance as shown in Fig. 24. 'Yielded' would be able to denote this state. The angle mentioned above is in the range of 45° to 55° in the interior of circular rod tensile specimens (Fig. 25), though about 55° on the surface similarly to the above.

These sharp X-type bands have not been observed in twisted specimens, but bands develop along the planes subjected to principal shearing stresses, long axially and around circumferentially (Fig. 9). The torque ceases its increase as soon as the bands begin to appear.

Fig. 15 shows the deformation bands obtained by a compression test of a specimen with concentric grooves at its end surfaces. Otherwise, without any stress concentration, we got no sharp deformation bands but such as shown in Fig. 17.

5. Principal Stresses and Equivalent Stress-Strain Relation.

The principal values of the true stresses at the maximum load are evaluated and given in Table 3, which are average values of the measurements of 5~15 specimens for each test. The eqivalent stresses $\bar{\sigma}$ and strains $\bar{\varepsilon}$ are calculated by the expression (5) for buldge tests and

$$\bar{\sigma} = \sqrt{3}\,\tau, \qquad \bar{\varepsilon} = \frac{1}{\sqrt{3}}\gamma, \tag{6}$$

Table 3.

Tests	Principal Stresses		Equivalent Stress (kg/mm²)	Equivalent Strain (%)
	σ_1 (kg/mm²)	σ_2 (kg/mm²)		
Internal Pressure	7.66	3.83	6.61	4.45
Tension	7.35	0	7.35	6.17
Compression	0	−7.31	7.31	8.34
Torsion	4.26	−4.26	7.37	8.90

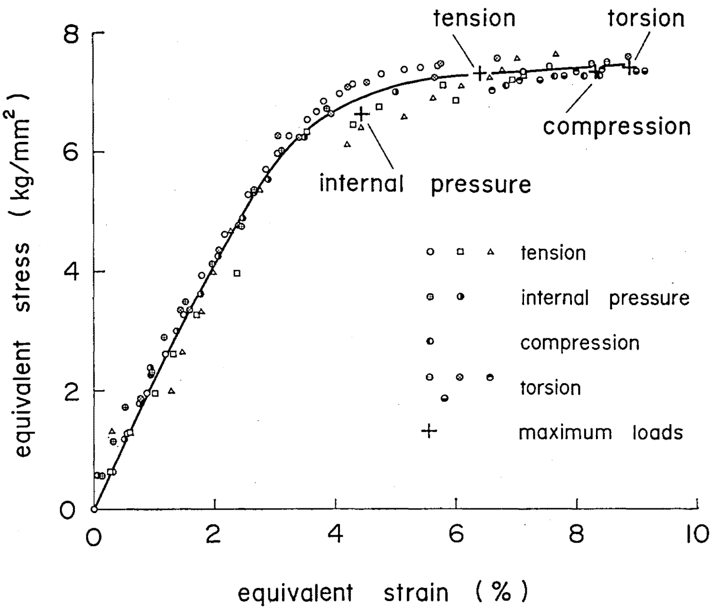

Fig. 26. Equivalent stresses vs. equivalent strains assembled and representation of instability points.

for torsion where τ is the shearing stress and γ the shearing strain. They are plotted together with those of tensile as well as compressive stresses in Fig. 26. They can be considered to lie on a curve regardless of the way of loading and the points of the maximum load are, dependently on their strain values, in the order of internal pressure, tension, compression and torsion. Whereas the maximum equivalent stresses do not quite differ from one another, their equivalent strains appreciably differ (Table 3). It also may be approved that hydrostatic pressure to the extent of 6~7 kg/mm^2 has only small effect on the stress-strain behavior of polycarbonate because the difference between twisting and internal pressure tests is not recognized in the equivalent values of stress and strain.

6. Discussions.

6-1 Mechanical and Material Instabilities.

Now we put an interpretation on the deformational process of polycarbonate material in terms of equivalent stress and strain, though they might not be the only concept for interpretation. Deformation bands formation itself is, according to Argon et al., another instability of molecular structural deformation, material instability differing from mechanical. Material instability is supposed to take place at an equivalent strain of 9 % for polycarbonate (Fig. 26).

It results from achievement of this strain that the load ceases from increasing in tests of homogeneous torsion and compression under monotonic increasing of deformation. In these cases no mechanical instability occurs without material instability.

In tension, however, mechanical instability occurs prior to material one, for the geometry of the stress-strain curve prescribes the onset at a strain of 6.2 %, being less than the strain of the material instability. A strain up to 6.2 % or so recovers viscoelastically. The strain of mechanical instability will vary with the form of the stress-strain curves according to materials, strain rate or other. Both the hollow cylinders and the grooved plates subjected respectively to internal pressure and to tension get to mechanical instability in the first place like in tension (Fig. 26). The localized tensile strain due to mechanical instability will acceleratively increase to the value of 9 %, at which the material structure becomes unstable and the material continues to deform in conjunction with deformation bands formation just as in torsion, until the deformation accomplishes the strain value of 70 %.

6-2 Yielding and Cold Drawing.

The temperature may rise with the strain increase at the necked section, but not so much as to prevent strain hardening, because the section would continue to neck until rupture but for hardenability. On load increase the bands develop and multiply, and the material yields. This is followed by hardening, which stops necking at the section and accompanies stress rise on the adjoining. Thus yielding propagates and the material cold-draws.

Stress raisers such as voids and inclusions in the material may have varying degrees of severity, i.e. weakness in material instability, and a small number of weaker ones may incipiently give rise to so few fine X-type deformation bands. Such is also the case with a notched specimen; our interpretation will be valid when a small specimen taken from the very portion including the defect site is tested.

Energy for producing the necked part has been evaluated from the load-extension curve together with the elongation of the necked part during cold-drawing, and is 4.43 kgmm/mm^3. Similarly 4.05 kgmm/mm^3 is obtained for torsion. These are one order less than the fracture energy of polymethyl methacrylate.[13]

6-3 Angles of Necking Direction and X-type Bands.

The direction of the neck and undulation (Fig. 17) due to instability, mechanical and in succession converted into material, are $59° \sim 63°$ and $26° \sim 30°$ for tensile and compressive tests respectively. Their sum is very near to 90°. These were not varied with a 2.5 mm thick plate specimen particularly prepared. However, the obtained hydrostatic pressure effect on yield stresses is so small that the criterion represented by the Coulomb-Navier equation may not be introduced to explain the magnitude of the angles. Here, compressibility of the material can be taken into consideration at the onset of instability, though the volume change has been said ignorable in the plastic stage of cold-drawing. Thomas [28] gave $\theta = 62°20'$, $61°17'$, $60°19'$ and $59°23'$ for tension with the values of Poisson's ratios $\nu = 0.275$, 0.300, 0.325 and 0.350 under the von Mises' yield condition. They are given for metals but seem available for polycarbonate having a value about 0.34 for ν.

This aspect removes a difficulty arising from accepting the Coulomb-Navier criterion, according to which the deformation bands would not advance along the maximum shearing stress planes even in simple torsion; whereas, deformation bands are produced along those planes in our cases as already denoted.

There is other difficulty; the angles of θ of deformation bands obtained of plate specimens with a small through hole of 0.3 mm and 1.0 mm diameter for each test are $47° \sim 50°$ and $44° \sim 47°$ for tension and compression respectively, which have been measured after removal of load and corrected to the loaded state; this is needed because of the low modulus of the polymer different from metals. The difference from the angles of bands given before will, however, be regarded as caused by the difference of the condition for the strain at the boundary of the hole; the material is free in two principal directions in this case.

There arises another difficulty; how can the incipient fine X-type bands appear with an angle of 55° to the direction of the load? Those bands can be treated as being made amidst an elastic vast because they grow in the early stage of loading. Assuming a value $\nu = 1/3$ for simplicity, we get $54°\,44'$ as an angle for the bands likely to form under the condition of strain to vanish.

6-4 Mechanical Instability in Torsion.

An instability shown in Fig. 10, being associated with a sudden decrease in diameter at a section seems to occur under a condition of large deformation. The necked region spreads steadily in succession and the specimen more or less elongates longitudinally, possibly because of large deformation of torsion but not because of anisotropy. On removal of torque, elongation is added; this now may be owing to anisotropy that has been produced by the inceptive plastic deformation.

7. Conclusion.

The mechanical behaviors of polycarbonate under statical load have been investigated at room temperature. The stress-strain curves obtained are well in accord with one another when they are represented with the equivalent stresses and strains.

The respective maximum loads are in the order of internal pressure, tension, compression and torsion on the curve. Consequently the values of equivalent strains at maximum load are in this order in magnitude, appreciably differing from one another while the equivalent stresses do not much.

Up to 6.2 % or less of equivalent tensile strain, the strain recovers; the instability caused at 6.2 % is mechanical; the critical value of the strain depends on materials by means of the form of the true stress-strain curves. As a result of this instability, the strain is quickly augmented to the extent of material instability. A strain as far as 9 % can not be recovered; in terms of equivalent strain, 9 % is supposed to be the value of the onset of material instability.

When there is strain concentration in the material, the above interpretation will be valid of the concentrating local strain. Development and multiplication of deformation bands are regarded as the period when the material has the largest probability for deformation bands initiation. Inceptive deformation bands produced before the mechanical instability are few and of fine X-type, and inclined about 55° to the direction of tensile stress, such as observed of the neck direction in mild steel.

Hydrostatic pressure dependence of the onset of mechanical instability is not so much as to make the Coulomb-Navier criterion applicable to the explanation of the measured neck direction of about 60°; but the von Mises' crietrion can account for it with the Poisson's ratio 0.34. On the other hand, the angle 55° of the above mentioned fine X-type deformation bands, which present themselves with their centers at flaws, can be deduced with the same value of Poisson's ratio from the condition that the precocious bands grow in a direction of strain to vanish.

The energy required for cold-drawing has been evaluated from the load-deformation curves together with the measurements of the increase in the necked length; 4.43 kgmm/mm^3 is for tension and 4.05 kgmm/mm^3 for torsion. These are one order less than the fracture energy of polymethyl methacrylate.

We wish to express our thanks to Mr. H. Ishii for help with the experiments and to Mr. M. Takenaka for preparing many test specimens and making measurement.

References

1) W. F. Christopher, D. W. Fox, Polycarbonates, Reinhold, New York (1962).
2) W. Hechelhammer, G. Peilstoecker, Kunststoffe, 49 (1959) 3.
3) R. E. Robertson, R. G. Buenker, J. Polymer Sci., Part A, 2 (1964) 4889.
4) R. A. Ekval, J. R. Low, J. Appl. Polymer Sci., 8 (1964) 1677.
5) R. E. Robertson, General Electric Report No. 64-RL-3794 C(1964).
6) J. P. Mercier, J. J. Aklonis, M. Litt, A. V. Tobolsky, J. Appl. Polymer Sci., 9 (1965) 447.
7) M. Higuchi, Reports of Res. Inst. Appl. Mech., Kyushu Univ., 16 (1968) 53.

8) T. Maeda, A. Makinouchi, Preprint of 42nd Ann. Meeting of Japan Soc. Mech. Engrs., 118 (1964) 95.
9) I. Marshall, A. B. Thompson, Proc. Roy. Soc., Ser. A, 221 (1954) 541.
10) P. I. Vincent, Polymer, 1 (1960) 7.
11) A. S. Argon, R. D. Andrews, J. A. Godrick, W. Whitney, J. Appl. Phys., 39 (1968) 1899.
12) H. Hyakutake, The 11th Japan Congr. Materials Research, (1968) 164.
13) e. g., M. Higuchi, Proc. 1st Intern. Conf. Fracture, II (1965) 1212.
14) A. Nadai, Theory of Flow and Fracture of Solids I, 316, McGraw-Hill, New York (1950).
15) R. J. Curran, R. D. Andrews, MIT Research Report R63-55 (1963).
16) J. K. Knowles, A. G. H. Dietz, Trans. Am. Soc. Mech. Eng., 77 (1955) 177.
17) M. Higuchi, Reports of Res. Inst. Appl. Mech., Kyushu Univ., 11 (1963) 39.
18) R. Hill, Mathematical Theory of Plasticity, 94, Clarendon Press, Oxford (1950).
19) N. Loizou, R. B. Sins, J. Mech. Phys. Solids, 1 (1953) 234.
20) R. Hill, J. Mech. Phys. Solids, 1 (1953) 271.
21) B. B. Hundy, A. P. Green, J. Mech. Phys. Solids, 3 (1954) 16.
22) G. Lianis, H. Ford, J. Mech. Phys. Solids, 5 (1957) 215.
23) J. P. Ellington, J. Mech. Phys. Solids, 6 (1958) 276.
24) H. Hyakutake, Preprint of 17th Ann. Meeting of Soc. Materials Sci., Japan (1968) 177.
25) R. Hill, Mathematical Theory of Plasticity, 17, Clarendon Press (1950).
26) W. Whitney, J. Appl. Phys., 34 (1963) 3633.
27) S. B. Newman, I. Wolock, J. Res. N. B. S., 58 (1957) 337.
28) T. Y. Thomas, Proc. N. A. S., 39 (1953) 266.

(Received October 18, 1968)